Available online at www.sciencedirect.com
ScienceDirect
Analytical Biochemistry 364 (2007) 122–127
ANALYTICAL BIOCHEMISTRY
www.elsevier.com/locate/yabio

Using cadmium telluride quantum dots as a proton flux sensor and applying to detect H9 avian influenza virus

Zhang Yun [a,b], Deng Zhengtao [c], Yue Jiachang [a,*], Tang Fangqiong [c], Wei Qun [b]

[a] National Laboratory of Biomacromolecules, Institute of Biophysics, Chinese Academy of Sciences, Beijing 100101, China
[b] Department of Biochemistry and Molecular Biology, Beijing Normal University, Beijing Key Laboratory, Beijing 100875, China
[c] Technical Institute of Physics and Chemistry, Chinese Academy of Sciences, Beijing 100080, China

Received 9 November 2006
Available online 3 March 2007

Abstract

Semiconductor nanocrystals, often known as quantum dots, have been used extensively for a wide range of applications in bioimaging and biosensing. In this article, we report that the pH-sensitive cadmium telluride (CdTe) quantum dots (QDs) were used as a proton sensor to detect proton flux that was driven by ATP synthesis in chromatophores. To confirm that these QD-labeled chromatophores were responding to proton flux pumping driven by ATP synthesis, *N,N′*-dicyclohexylcarbodiimide (DCCD) was used as an inhibitor of ATPase activity. Furthermore, we applied the QD-labeled chromatophores as a virus detector to detect the H9 avian influenza virus based on antibody–antigen reaction. The results showed that this QD virus detector could be a new virus-detecting device.

Keywords: Proton flux; Quantum dots; F_0F_1–ATPase; ATP synthesis; H9 avian influenza virus

Semiconductor quantum dots (QDs),[1] also called semiconductor nanocrystals [1], are roughly spherical and generally composed of atoms from groups II and VI (e.g., cadmium selenide [CdSe], cadmium sulfide [CdS], cadmium telluride [CdTe]) or groups III and V (e.g., indium phosphide [InP]) of the periodic table. The diameters of QDs typically are between 1 and 10 nm, and each dot contains a relatively small number of atoms in a discrete cluster [2]. Interestingly, the electronic properties of QDs differ significantly between bulk semiconductor and nanocrystals of the same material as a result of quantum confinement effects in the QDs [2–5]. Consequently, QDs have an exploitable property on irradiation. Energy is absorbed (at any wavelength greater than the energy of QDs' lowest energy transition) and converted into an extremely narrow bandwidth emission close to the band edge [6–8]. The unique photophysical properties of QDs provide a new class of biological labels that could overcome the limitations of conventional organic fluorophores. Stability against photobleaching [9], large molar extinction coefficients, high quantum yield [10], and large surface/volume ratios make QDs superior to organic fluorophores in detection sensitivity as well as in luminescent stability.

For these advantages of QDs, many researchers have used QDs as signal reporters conjugated with biomaterial. It has been reported that aqueous compatible, silanized CdSe/CdS were labeled with cell nuclei via electrostatic and hydrogen bonding interactions with trimethoxysilylpropyl urea [11]. Later, Zhang and coworkers [12] demonstrated that 3-mercaptopropyl acid-stabilized CdTe QDs synthesized in aqueous solution could be effectively bound

* Corresponding author. Fax: +86 10 64871293.
E-mail address: yuejc@sun5.ibp.ac.cn (Y. Jiachang).

[1] *Abbreviations used:* QD, quantum dot; CdSe, cadmium selenide; CdS, cadmium sulfide; CdTe, cadmium telluride; InP, indium phosphide; F-DHPE, *N*-(fluorescein-5-thiocarbamoyl)-1,2-dihexadecanoyl-*sn*-glycero-3-phosphoethanolamine; DCCD, *N,N′*-dicyclohexylcarbodiimide; TGA, thiolglycolic acid; $TF_1\beta$, thermophilic bacterium *Bacillus* PS3 β-subunit; PBS, phosphate-buffered saline.

0003-2697/$ - see front matter © 2007 Elsevier Inc. All rights reserved.
doi:10.1016/j.ab.2007.02.031

to a biomacromolecule, papain, via electrostatic interaction. More recently, QDs were used to compose a mechanism to probe changes of pH with pronounced fluorescence changes [13]. Another report described how mercaptoacetic acid-capped CdSe QDs were influenced by pH [14]. These reports indicate that QDs have some relationship with the concentration of proton. However, limited information about the application of pH sensitivity of QDs has been published.

The F_0F_1–ATP synthase is a nanoscale rotary biological motor. Cui and coworkers [15] labeled *N*-(fluorescein-5-thiocarbamoyl)-1,2-dihexadecanoyl-*sn*-glycero-3-phosphoethanolamine (F-DHPE) on the surface of chromatophores to detect proton flux through F_0F_1–ATPase driven by ATP hydrolysis. Based on their experiment, Liu and coworkers [16] devised a biosensor to detect single virus.

In this context, we describe the pH sensitivity of CdTe QDs and successfully label QDs on the surface of chromatophores to monitor proton flux. Furthermore, we use these QD-labeled chromatophores to construct a novel QD virus detector for detecting the H9 avian influenza virus.

Materials and methods

Materials

N,N′-Dicyclohexylcarbodiimide (DCCD) and ADP were purchased from Sigma–Aldrich (USA). All other analytically purified reagents were of analytical grade.

Synthesis of water-soluble CdTe QDs

The CdTe QDs were synthesized via a modified protocol that was adopted from the literature by adding freshly prepared NaHTe solution to nitrogen-saturated $Cd(NO_3)_2$ solutions at pH 8.5 in the presence of thiolglycolic acid (TGA) as a stabilizing agent. A small amount of ammonia was added in the solution as an additional stabilizing agent and pH controller because this would enable us to obtain high-quality QDs with a smaller size and a higher quantum yield. A series of QDs with sizes ranging from 2 to 5 nm were obtained, and in this work we used QDs with a maximum emission wavelength of 535 nm.

Labeling of QDs on the outside surface of chromatophores

Chromatophores were prepared from the cells of *Rhodospirillum rubrum* according to Refs. [17,18]. The suspension of chromatophores (100 μl) was centrifuged at 13,000 rpm for 30 min at 4 °C to wash away the glycerol. The precipitate was resuspended in buffer A (50 mM tricine–NaOH, 5 mM $MgCl_2$, 10 mM KCl, pH 6.5) and incubated for 3 h at room temperature after adding 100 μl CdTe QDs (1×10^{15}/μl, dissolved in water). Free QDs were washed away by centrifuging at 13,000 rpm for 30 min at 4 °C three times. The precipitate (QD-labeled chromatophores) was resuspended in 100 μl of 50 mM tricine buffer (pH 6.5) and stored at 4 °C before use.

Preparation of antithermophilic bacterium Bacillus PS3 β-subunit antibody

The β-subunit of F_0F_1–ATPase from thermophilic bacterium *Bacillus* PS3 ($TF_1\beta$) was expressed in *Escherichia coli* JM103 [19] and purified as in Ref. [20]. The antibody was prepared according to Ref. [21]. The antibody was purified by precipitation with 33% $(NH_4)_2SO_4$ and stored at –20 °C before use.

Preparation of H9 avian influenza virus

The H9 influenza A viruses were propagated in the allantoic cavities of 11-day-old embryonated chicken eggs at 37 °C for 3 days. The allantoic cavities were collected and centrifuged at 4000 rpm for 40 min, and then the supernatant was centrifuged again at 100,000 *g* for 2 h. The viruses were resuspended in phosphate-buffered saline (PBS) buffer and used in the following experiments [22]. The H9 influenza A and H9 influenza A antibodies were obtained from Ni Zhiqian (Harbin Veterinary Research Institute, Harbin, China).

Constructing the QD virus detector

Here 2 μl of 2 μM biotin was added in 20 μl β-subunit antibody and incubated for 30 min at room temperature, followed by adding 2 μl of 2 μM streptavidin and incubating for 30 min at room temperature. The biotin-streptavidin-labeled β-subunit antibody was added to 100 μl QD-labeled chromatophores and incubated for 1 h at 37 °C. Redundant free β-antibody was washed by centrifuging at 13,000 rpm for 10 min three times. Then 15 μl H9 avian influenza virus antibody, after being incubated with 2 μl of 2 μm/ml biotin for 30 min at room temperature, was added. Free antibody was washed by centrifuging at 13,000 rpm for 10 min three times. The prepared QD virus detectors were resuspended in 100 μl of 0.1 mM tricine buffer (pH 8.0) and stored at 4 °C.

Fluorescence assay

ADP was dissolved in 1 ml ATP synthesis buffer (0.1 mM tricine, 5 mM $MgCl_2$, 5 mM K_2HPO_4, 10% glycerol, pH 8.0) with a final concentration of 4 mM. Then 100 μl QD virus detectors was added and incubated for 5 min at 37 °C. The fluorescence changes of QD virus detectors were recorded by an F-4500 fluorescence instrument (Hitachi, Japan) for 900 s at 37 °C. Fluorescence was excited at 488 nm and registered at 535 nm. All experimental data were obtained from at least four to six independent tests.

Results and discussion

Relationship between fluorescence intensity of CdTe QDs and pH values

In our experiment, we noticed that water-soluble CdTe QDs are sensitive to pH changes. Photoluminescence measurement of QDs in indicated pH buffers (6.0, 6.5, 7.0, 7.5, 8.0, and 9.0) was performed by the F-4500 fluorescence instrument with an excitation wavelength at 488 nm. As can be seen in Fig. 1A, the fluorescence intensity of QDs with the maximum emission wavelength at 535 nm increased with decreasing pH values. Fig. 1B illustrates the peak fluorescence intensity of each curve. The results show the linear relationship between fluorescence intensity of CdTe QDs and pH values from 8.0 to 6.0, so a pH value of 8.0 was chosen for the following tests.

Using QD-labeled chromatophores to detect proton flux driven by ATP synthesis

Because of the electrostatic effect, QDs can readily attach to the surface of chromatophores. These noncovalent conjugations were very steady and did not influence the fluorescence of QDs. To confirm the existence of QDs on the surface of chromatophores, a kind of QD fluorescence quencher should be used. In our experiment, the well-known fluorescence quencher Cu^{2+} was attempted. As shown in Fig. 2A, when 10 μl QDs was added to 3 ml tricine buffer, the fluorescence intensity was remarkably higher than that of tricine buffer as the control (curve a vs. curve c). However, after the addition of 1 mg/ml $CuCl_2$, the fluorescence intensity of QDs was as low as the control (curve b vs. curve c). The results indicate that Cu^{2+} is a valid fluorescence quencher of QDs. Then we used the 1 mg/ml $CuCl_2$ to test the conjugation. Fig. 2B shows the fluorescence intensity changes of QD-labeled chromatophores when $CuCl_2$ was added. The fluorescence intensity of QD-labeled chromatophores (curve a) was higher than that of chromatophores as the control (curve c) even though it was washed by centrifugation several times. However, the fluorescence intensity decreased rapidly when 1 mg/ml $CuCl_2$ was added (curve b). This result indicated that $CuCl_2$ quenched the fluorescence of QDs, which were really labeled to the outer surface of chromatophores. These QD-labeled chromatophores provided us with a proton detector for the following application.

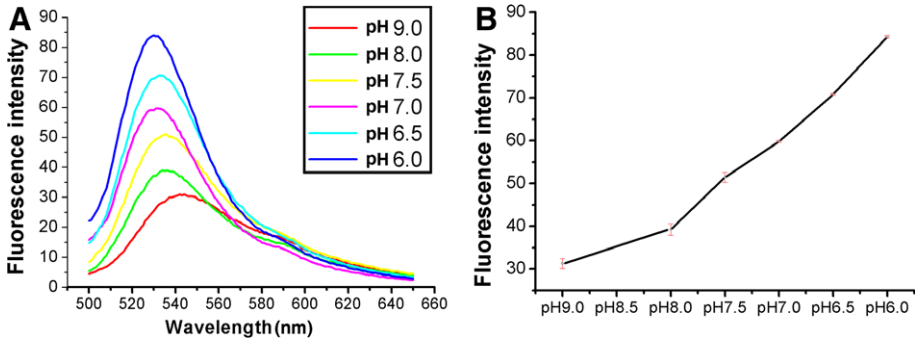

Fig. 1. Relationship between fluorescence intensity of QDs and pH values. (A) Spectrum of CdTe QDs in indicated pH buffer. Here 20 μl CdTe QDs was added into 2 ml tricine (50 mM) with various pH values (6.0, 6.5, 7.0, 7.5, 8.0, and 9.0). Photoluminescence measurement of QDs was excited at 488 nm and scanning from 500 to 650 nm. (B) Peak fluorescence intensity of each curve.

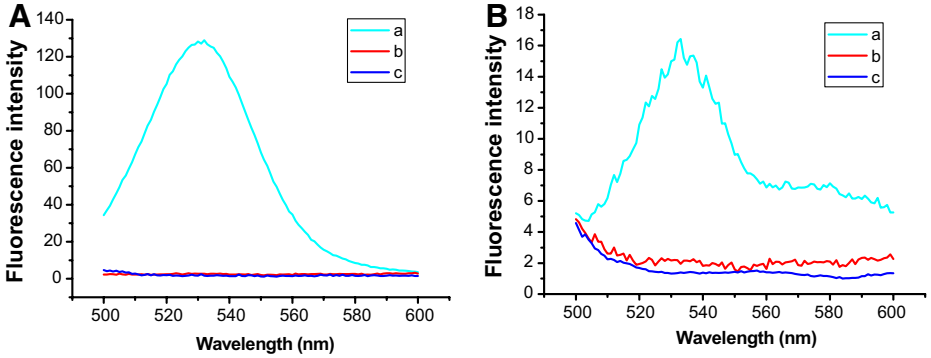

Fig. 2. Using Cu^{2+} to confirm the existence of QDs on the surface of chromatophores. (A) Cu^{2+} as a valid fluorescence quencher of QDs: (a) 10 μl QDs was added to 3 ml tricine buffer (50 mM, pH 6.5) with excitation at 488 nm; (b) 10 μl $CuCl_2$ (1 mg/ml) was added to sample; (c) fluorescence intensity of tricine buffer as control. (B) Testing the labeling of QDs using Cu^{2+}: (a) fluorescence intensity of QD-labeled chromatophores (20 μl) dissolved in 3 ml tricine buffer (50 mM, pH 6.5) with excitation at 488 nm; (b) 10 μl $CuCl_2$ (1 mg/ml) was added to sample; (c) fluorescence intensity of chromatophores as control.

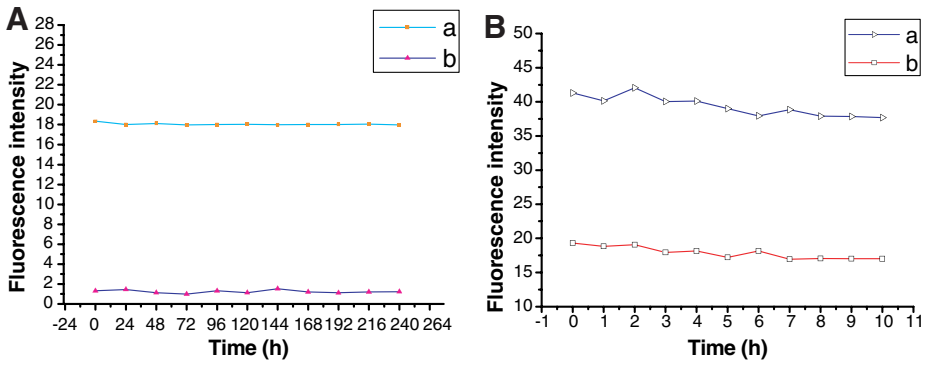

Fig. 3. Tests of the physical and fluorescent stability of QD-labeled chromatophores. (A) Physical stability of QD-labeled chromatophores: (a) fluorescence intensity of QD-labeled chromatophores after storing at 4 °C (for 0, 24, 48, 72, 96, 120, 144, 168, 192, 216, and 240 h); (b) fluorescence intensity of tricine buffer as control. (B) Fluorescent stability of QD-labeled chromatophores: (a) fluorescence intensity of QDs after being excited at 488 nm with 150-W Xe lamp for 0, 1, 2, 3, 4, 5, 6, 7, 8, 9, and 10 h as control; (b) fluorescence intensity of QD-labeled chromatophores after being excited at 488 nm with 150-W Xe lamp for 10 h.

Furthermore, the physical and fluorescent stability of QD-labeled chromatophores was tested and is shown in Fig. 3. Fig. 3A shows that the fluorescence of QD-labeled chromatophores had no obvious change (curve a) after 240 h of storing at 4 °C. As shown in Fig. 3B, QD-labeled chromatophores (curve b) showed a capability of high photostability similar to that of the QDs (curve a).

As we know, F_0F_1–ATPase is the universal enzyme that synthesizes ATP. When the ATP is synthesized, the protons are pumped out of chromatophores and subsequently result in an increase of concentration of H^+ in the solution. Thus, the pH will decrease in a solution of 0.1 mM tricine with poor buffer capacity, and the pH-sensitive QDs are expected to detect the pH decrease by recording the fluorescence intensity.

Furthermore, DCCD is an F_0 channel inhibitor, and this can inhibit the ATPase activity of chromatophores and block the proton pump; therefore, it can be used to confirm that the fluorescence intensity change of the QDs was really caused by the proton flux out of the chromatophores. As shown in Fig. 4, when 4 mM ADP was added to initialize the reaction at 37 °C, the fluorescence intensity increased, indicating an increase of pH value near chromatophores (curve a), whereas QD-labeled chromatophores incubated with 2 μM DCCD previously showed no obvious change of fluorescence intensity (curve b). The fluorescence intensity changes of QD-labeled chromatophores without adding ADP was the control. Because of the lack of ADP, ATP could not be synthesized and few protons were pumped out of chromatophores; consequently, the fluorescence of QDs had no obvious changes (curve c). The results showed that the increasing fluorescence intensity was coupled with ATP synthesis activity and proton flux.

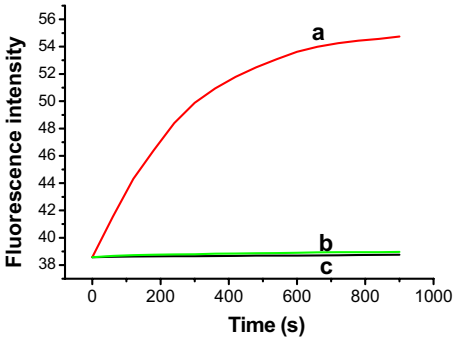

Fig. 4. Effect of inhibitor on fluorescence intensity changes of QD-labeled chromatophores. Curve a: fluorescence intensity changes of QD-labeled chromatophores when 4 mM ADP was added to initialize reaction. Curve b: QD-labeled chromatophores incubated with 2 μM DCCD for 1 h at room temperature previously when 4 mM ADP was added to initialize reaction. Curve c: fluorescence intensity changes of QD-labeled chromatophores without adding ADP as control.

Construction and application of QD virus detector

As mentioned above, when the F_0F_1–ATPase synthesized ATP, the velocity of the proton pump could be

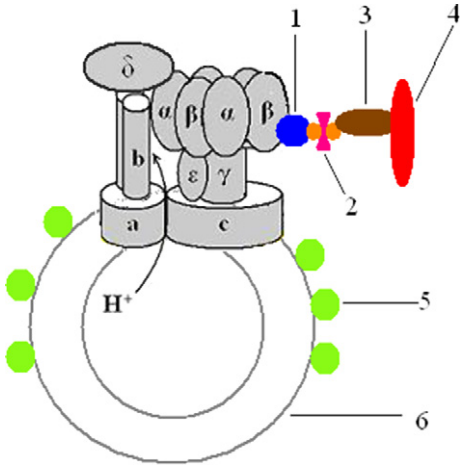

Fig. 5. Basic design of QD virus detector based on F_0F_1–ATPase antibody of β-subunit (1), the system of biotin-streptavidin-biotin (2), the antibody of H9 avian influenza virus (3), H9 avian influenza virus (4), 535 nm QDs (5), and chromatophores with F_0F_1–ATPase (6). The "a,b,c" and "α,β,γ,ε,δ" represent subunits of F_0F_1–ATPase. And the "H^+" represent protons.

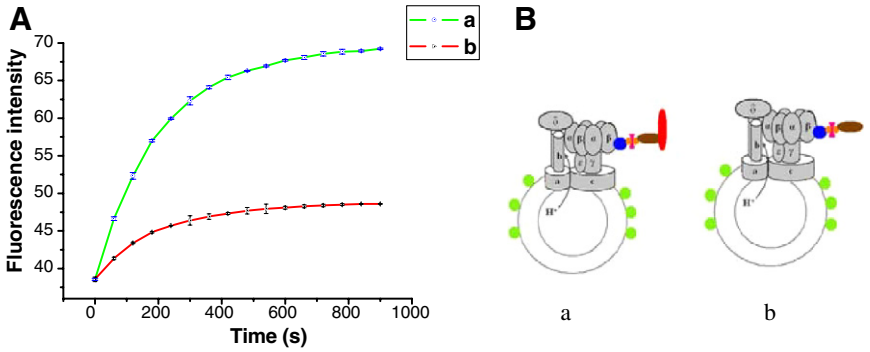

Fig. 6. Effects of H9 virus on ATP synthesis activity of F_0F_1–ATPase. (A) Fluorescence intensity changes of QD virus detector, either virus loaded or not virus loaded, during ATP synthesis. Curve a: QD virus detector with capturing virus. Curve b: QD virus detector without capturing virus. (B) Schematic view of QD virus detector during ATP synthesis. Left image: QD virus detector with capturing virus. Right image: QD virus detector without capturing virus. The "a,b,c" and "α,β,γ,ε,δ" represent subunits of F_0F_1–ATPase. And the "H^+" represent protons.

reflected by measuring the fluorescence changes of QDs labeled on the outer surface. So, the fluorescence of QDs was related with the ATP synthesis activity. Moreover, according to the rotational catalysis mechanism [23], the rotation of the central γεcn rotor relative to the $\alpha_3\beta_3$ hexagon is critical for operation of the catalytic sites, and the rotation of γεcn relative to the β-subunit is critical for proton transport during ATP synthesis. It has been reported that various molecules loading to the β-subunit can affect the ATP synthesis activity of F_0F_1–ATPase [16]; therefore, the change of QD fluorescence can also reflect various loadings of the β-subunit. Based on this principle, we designed a QD virus detector using the F_0F_1–ATPase shown in Fig. 5. The F_1 β-subunit site of F_0F_1–ATPase linked to a β-antibody-biotin-streptavidin-biotin-antibody system (especially for the avian virus) was used as a capture reaction receptor. After capturing virus on the β-subunit, the ATP synthesis activity of F_0F_1–ATPase changes, resulting in the rate of the QD fluorescence increase changing more evidently. As shown in Fig. 6, when 4 mM ADP was added to the reaction buffer, the fluorescence of the virus-loaded detector (Fig. 6A curve a) changed more evidently compared with that of the non-virus-loaded detector (Fig. 6A curve b). And Fig. 6B showed the Schematic view of QD virus detector during ATP synthesis. The result shows that the fluorescence of the QD virus detector increased more rapidly after capturing the virus, with the possible mechanism being that different load weights will affect the conformation of the β-subunit, but the exactly mechanism is still under discussion. Although it is unclear how it occurs in detail, the application of the QD virus detector, as a proton flux indicator and a virus detector, is vital to routine inspection. Furthermore, because QDs show size-tunable fluorescence emission and have a narrow and symmetric spectral line profile (the full-width half maximum typically is 25–35 nm) compared with that of organic dyes [24,25], it is possible to develop an encoded method using the QD virus detector for detecting various viruses simultaneously.

Conclusion

In this study, a new application of QDs as proton sensor has been achieved preliminarily. We showed that QDs have a potential application for detecting ATP-driven proton-pumping activity of F_0F_1–ATPase and proton translocation across F_0 driven by proton-motive force. Based on these properties, we devised a QD virus detector and successfully captured the H9 avian influenza virus. Moreover, because of its unique optical properties and exceptional photostability of QDs, the QD virus detector may have a wide range of applications in the future.

Acknowledgments

This work was granted by programs of the Natural Science Foundation of China (30292905, 90306005, 20545002, 60572031, and 60372009) and nanobiomedical and device application of CAS (Kjcx-sw-h12).

References

[1] C.M. Niemeyer, Nanoparticles, proteins, and nucleic acids: Biotechnology meets materials science, Angew. Chem. Intl. Ed. Engl. 40 (2001) 4128–4158.
[2] C.B. Murray, C.R. Kagan, M.G. Bawendi, Synthesis and characterisation of monodisperse nanocrystals and close packed nanocrystal assemblies, Annu. Rev. Mater. Sci. 30 (2000) 545–610.
[3] M. Green, P. O'Brien, Recent advances in the preparation of semiconductors as isolated nanometric particles: New routes to quantum dots, J. Chem. Soc. Chem. Commun. 22 (1999) 2235–2241.
[4] A.P. Alivisatos, Semiconductor clusters, nanocrystals, and quantum dots, Science 271 (1996) 933–937.
[5] C.J. Murphy, J.L. Coffer, Quantum dots: A primer, Appl. Spectrosc. 56 (2002) 16A–27A.
[6] L.E. Brus, Electron–electron and electron–hole interactions in small semiconductor crystallites: The size dependence of the lowest excited electronic state, J. Chem. Phys. 80 (1984) 4403–4409.
[7] L. Spanhel, M. Haase, H. Weller, A. Henglein, Surface modification and stability of strong luminescing CdS particles, J. Am. Chem. Soc. 109 (1987) 5649–5655.

[8] C.B. Murray, D.J. Norris, M.G. Bawendi, Synthesis and characterization of nearly monodisperse CdE (E = sulfur, selenium, tellurium) semiconductor nanocrystallites, J. Am. Chem. Soc. 115 (1993) 8706–8715.
[9] X.Y. Wu, H.J. Liu, J.Q. Liu, K.N. Haley, J.A. Treadway, J.P. Larson, N.F. Ge, F. Peale, M.P. Bruchez, Immunofluorescent labeling of cancer marker Her2 and other cellular targets with semiconductor quantum dots, Nat. Biotechnol. (2003) 2141–2146.
[10] W.C. Chan, S. Nie, Quantum dot bioconjugates for ultrasensitive nonisotopic detection, Science 281 (1998) 2016–2018.
[11] J.M. Bruchez, M. Moronne, P. Gin, S. Weiss, A. Alivisatos, Semiconductor nanocrystals as fluorescent biological labels, Science 281 (1998) 2013–2016.
[12] B.L. Zhang, S.X. Cui, H. Zhang, Q.D. Chen, B. Yang, X.G. Su, J.H. Zhang, Q.H. Jin, Studies on quantum dots synthesized in aqueous solution for biological labeling via electrostatic interaction, Anal. Biochem. 319 (2003) 239–243.
[13] M. Tomasulo, I. Yildiz, F.M. Raymo, pH-sensitive quantum dots, J. Phys. Chem. B 110 (2006) 3853–3855.
[14] Y.H. Sun, Y.S. Liu, P.T. Vernier, C.H. Liang, S.Y. Chong, L. Marcu, M.A. Gundersen, Photostability and pH sensitivity of CdSe/ZnSe/ZnS quantum dots in living cells, Nanotechnology 17 (2006) 4469–4476.
[15] Y.B. Cui, F. Zhang, J.C. Yue, Detecting proton flux across chromatophores driven by F_0F_1–ATPase using *N*-(fluorescein-5-thiocarbamoyl)-1,2-dihexadecanoyl-sn-glycero-3-phosphoethanolamine, triethylammonium salt, Anal. Biochem. 344 (2005) 102–107.
[16] X.L. Liu, Y. Zhang, J.C. Yue, P.D. Jiang, Z.X. Zhang, F_0F_1–ATPase as biosensor to detect single virus, Biochem. Biophys. Res. Commun. 342 (2006) 1319–1322.
[17] Z. Gromet-Elhanan, D. Khanashvili, Selective extraction and reconstitution of F_1 subunits from *Rhodospirillum rubrum*: Purification and properties of a reconstitutively active single subunit, Methods Enzymol. (1986) 528–538.
[18] S. Philosoph, A. Binder, Z. Gromet-Elhanan, Coupling factor ATPase complex of *Rhodospirillum rubrum*, J. Biol. Chem. 252 (1977) 8747–8752.
[19] C. Montemagno, G.D. Bachand, Constructing nanomechanical devices powered by biomolecular motors, Nanotechnology 10 (1999) 225–231.
[20] Y.H. Zhang, J. Wang, Y.B. Cui, J.C. Yue, X.H. Fang, Rotary torque produced by proton motive force in F_0F_1 motor, Biochem. Biophys. Res. Commun. 331 (2005) 370–374.
[21] W.C. Hanley, J.E. Artwohl, B.T. Bennett, Review of polyclonal antibody production procedures in mammals and poultry, ILAR J. 37 (1995) 93–118.
[22] A. Ninomiya, A.T. Katsunori, K. Okazaki, F. Shortridge, K. Hiroshi, Seroepidemiological evidence of avian H4, H5, and H9 influenza A virus transmission to pigs in southeastern China, Vet. Microbiol. 88 (2002) 107–114.
[23] P.D. Boyer, The ATP synthase: A splendid molecular machine, Annu. Rev. Biochem. 66 (1997) 717–749.
[24] S.J. Rosenthal, Bar-coding biomolecules with fluorescent nanocrystals, Nat. Biotechnol. 19 (2001) 621–622.
[25] Z. Tang, N.A. Kotov, M. Giersig, Spontaneous organization of single CdTe into luminescent nanowires, Science 297 (2002) 237–240.